SIZE-FREQUENCY DISTRIBUTION OF THE EJECTED BOULDERS SURROUNDING THE LINNE' CRATER (MOON).
Maurizio Pajola[1], Riccardo Pozzobon[2], Alice Lucchetti[1], Sandro Rossato[2], Emanuele Baratti[3], Valentina Galluzzi[4], Gabriele Cremonese[1], [1]INAF-Astronomical Observatory of Padova, Vic. Osservatorio 5, 35122 Padova, Italy (maurizio.pajola@inaf.it); [2]Geosciences Department, University of Padova, Padova, Italy; [3]Department of Civil, Chemical, Environmental and Material Engineering, University of Bologna, Bologna, Italy; [4]INAF-Istituto di Astrofisica e Planetologia Spaziali, Roma, Italy.

Introduction: The first boulders discovered on a non-terrestrial surface were observed on the Moon in 1965, thanks to the Ranger probe photographs [1]. In 1977, the Viking spacecraft photographed the first Martian boulders [2], hence suggesting that they might be present on other solid planetary surfaces too. Afterwards, by means of an increasing number of high resolution images of different Solar System targets it has become clear that boulders surrounding impact craters are present not only on the surface of the Earth [3], Moon [4] or Mars [5], but also on icy satellites [6], asteroids [7], as well as on the actively reshaping cometary surfaces [8]. By studying the boulder size-frequency distribution (SFD) it is possible to investigate a wide range of processes that occurred or are still occurring on a planetary/minor body surface. Indeed, boulders are the remnant of the excavated rocky interiors showing the underlying mineralogical composition [9] and their SFD, as well as the maximum generated sizes, are directly related to the impactor composition and velocity, to the impact site morphological, geological and mechanical properties. For the Moon's case, the study of the boulder SFD identified on different maria is a fundamental mean to study the distribution and layering thickness of the lunar volcanic basalts [10] and the superimposed regolith thickness present at the impact site [11].

The Linné crater: The Linné crater is located at 27.74° latitude and 11.8° longitude in northwestern Mare Serenitatis, a basaltic smooth basin located on the nearside of the Moon (Fig. 1). It is a simple crater with a diameter D of 2.194 km, a depth d of 0.52 km and a d/D ratio of 0.237 [12]. It likely formed in the late Copernican period, within the last 10 Ma [13], and lays on top of a complex stratigraphic sequence of distinct volcanic events that piled up to form an homogeneous unit, as shown in the geological map reported by [10]. The Mare Serenitatis stratigraphic sequence is characterised by piled up lava flows that could reach a few kilometers of depth from the maria surface, and each of these geological units can be up to several hundred metres thick [14].

In order to identify and map the ejected boulders surrounding the Linné crater we used two publicly available (http://wms.lroc.asu.edu/lroc/) Lunar Reconnaissance Orbiter Camera (LROC) mosaics made of two Narrow Angle Camera (NAC, [15]) images each characterised by a spatial resolution ranging between 1.1-1.3 m. For the global boulder SFD analysis, we considered a circular area with a radius of 5.3 km outside the craters' rim, i.e. 6.4 km from the crater's centre (Fig. 2A). Beyond this distance the identifiable boulders are so few that a statistical analysis would be hardly meaningful. Over this area, 124.01 km^2 wide, we identified 46273 boulders ≥2.2 m, 12067 of which being ≥4.4 m (i.e. 4 pixels). The corresponding density of boulders ≥4.4m per km^2 is 137.85. To understand

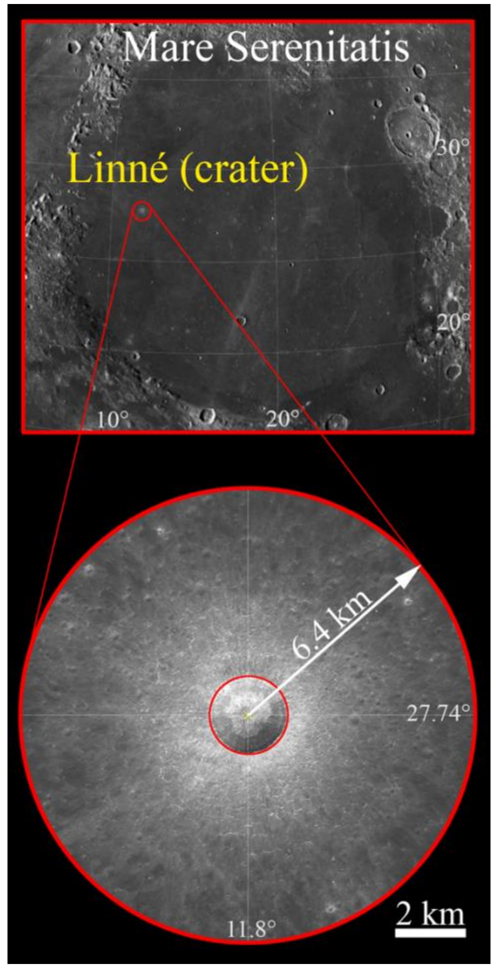

Figure 1: Context image showing the location of the Linné crater (2.2 km diameter, centred at 27.74° latitude, 11.8° longitude) in the Mare Serenitatis.

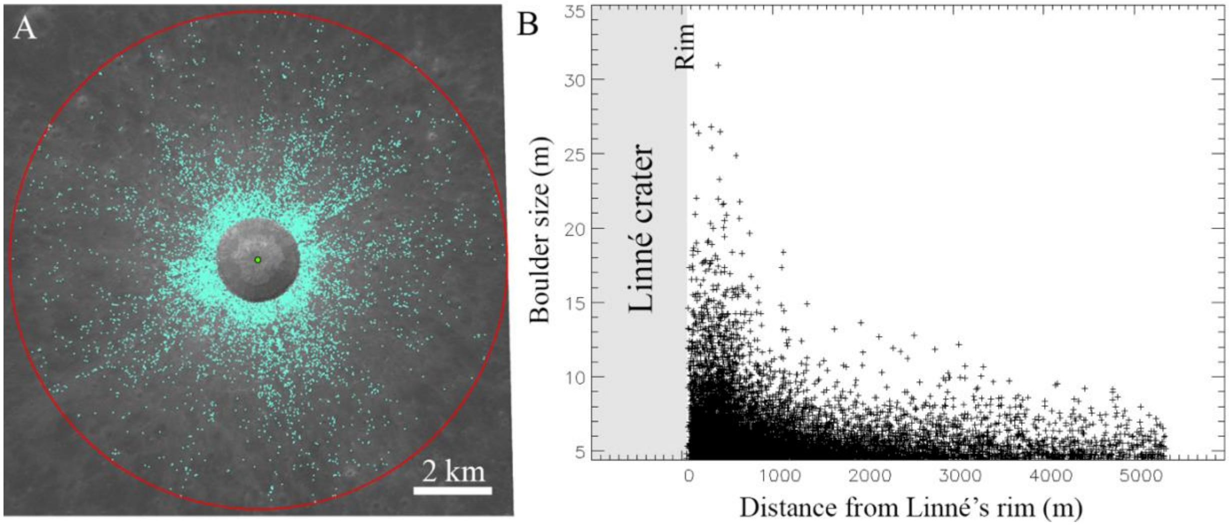

Figure 2: A) The spatial distribution of the identified ejected boulders ≥4.4 m on the study area (124.01 km^2). B) The boulder size versus distance distribution surrounding the Linné's crater.

how the boulder sizes are radially distributed from the Linné's rim we prepared the plot of Fig. 2B. As it is expected from impact cratering dynamics [16], the biggest sizes (>15 m) are all located in close proximity to the crater's rim, while their frequency radially decreases with increasing distances from the rim. At distances >3.5 km from the Linné's rim the ejected boulders are all <10 m in size. By studying the radial ejecta abundances, we found that, as the distance from Linné's rim increases, the boulder SFD power-law index steepens, ranging from -3.42 in the first 500 m to -3.82 at distances 10 times larger. This means that the relative abundance of the biggest sizes is largest within the first km from the rim, hence resulting in a shallower power-law index. On the other hand, at bigger distances the relative abundances of the smaller boulder sizes increases, becoming dominant with respect to the full statistics and hence steepening the SFD.

The Linné high-resolution geological map we prepared shows that its proximal ejecta blanket is slightly asymmetrical in the NE-SW direction. This is confirmed by our boulder surface density analysis. Such behaviour can be either the result of an oblique impact emplacement of the original impactor, that ejected more boulders in the impact direction causing this preferential distribution, or the result of a perpendicular impact in the Mare Serenitatis location, but on a surface characterised by an interface between maria basalts with different local mechanical properties. We consider both scenarios equally likely to explain the ejecta distribution anisotropies we observe.

Eventually, we investigated the possible relation between the boulders ejecta distribution and the regolith thickness at the Linné impact site, since local variations of such blanket may affect the boulders' travel distance [11]. By exploiting our boulders statistics and our Linné geological map, coupled with Eq. 9 of [11], we estimated that the corresponding regolith thickness at the Linné impact site should be ~4.75 m [17], hence supporting the previously indicated Mare Serenitatis' evaluations [18].

Acknowledgments: This Paper is part of a project that has received funding from the European Union's Horizon 2020 research and innovation programme under grant agreement Nº776276 (PLANMAP). We gratefully acknowledge the NASA LROC Archive node for providing access to the LROC dataset used in this work.

References: [1] Kuiper, G.P., 1965. The Johns Hopkins Press, 99. [2] Binder, A.B. et al., 1977. JGR 82, 4439. [3] Senthil Kumar, P. et al., 2014. JGR Planets 119, 2029. [4] Cintala, M.J., McBride, K.M., 1995. NASA Technical Memorandum 104804. [5] Moore, H.J., Jakosky, B.M., 1989. Icarus 81, 164. [6] Martens, H.R. et al., 2015. Icarus 245, 162. [7] Michikami, T. et al., 2008. EPS 60, 13. [8] Pajola, M. et al., 2015. A&A. 583, A37. [9] Shoemaker, E.M., 1987. Meteor Crater, Arizona, GSA Field Guide - Rocky Mountain Section. [10] Hiesinger, H. et al., 2000. JGR Planets 105, 29239. [11] Bart, G.D., Melosh, H.J., 2010. JGR 115 (Issue E8). [12] Garvin, J.B. et al., 2011. LPSC 42 #2063. [13] Stickle, A.M. et al. 2016. Icarus 273, 224. [14] Weider, S.Z. et al. , 2010. Icarus 209, 323. [15] Klem, S.M. et al., 2014. LPSC 45 #2885. [16] Melosh, H.J., 1989. Impact Cratering. Oxford Univ. Press, New York, p. 245. [17] Pajola, M. et al. 2019, PSS, in press: https://doi.org/10.1016/j.pss.2018.11.008. [18] Shkuratov, Y.G., Bondarenko, N.V., 2001. Icarus 149, 329.